Modeling of Terrains for Simulation of Integrated Mobile Terrestrial and Satellite Communications Systems

Gunar Schorcht, Ulrich Freund, Horst Salzwedel and Harald Keller

Faculty for Computer Science and Automation
Technical University of Ilmenau
E-mail: {Schorcht, Freund, Horst, Keller}@TheoInf.TU-Ilmenau.DE

Abstract - In this paper we present methods to generate models of mountainous regions. For these regions statistical methods are unsuitable to predict the service coverage, blocking and termination probabilities for systems involving fast moving satellites. We present methods using modeled terrains to analyze the service coverage in satellite integrated mobile communications systems. Results of service coverage analyses based on these methods are presented for proposed non-geostationary satellite systems.

I. INTRODUCTION

In third generation mobile communications systems hierarchical cell structures will be used. Hierarchical cell structures include cells at several levels, e.g., pico, micro, macro and umbrella cell level. Satellites are capable to serve large regions. Therefore, their integration with terrestrial systems enables the realization of umbrella cells in regions with sparse population and the realization of global coverage. Satellites in non-geostationary orbits are most suitable for this integration due to their lower power requirements and smaller round-trip-delays than satellites in geostationary orbits. However, the usage of non-geostationary satellites leads to dynamic cell constellations and therefore to continuously changing environmental conditions for mobile stations. Due to these dynamics, it is difficult to predict important system design parameters like service coverage, call blocking and undesired call termination probabilities. In regions where the line of sight to satellites is often distorted by large natural obstacles, it is important to know which part of the region can be covered by satellites and which have to be covered by terrestrial components. The service coverage is mainly influenced by signal level received at the mobile station. Therefore, the prediction of the signal level is one of the most important issues for estimating the system design parameters. References [1, 2, 3, 4] propose several statistical models for signal level prediction in satellite systems based on log-normal distribution for long-term fading, and Rayleigh and Rician distributions for short-term fading, respectively. Their parameters are defined by a few terrain classes. However, these models describe only the statistical properties of the signal level. They cannot predict the temporal signal level for given locations in a region. In such cases deterministic geometrical methods like the geometric diffraction theory *GTD* are suitable for signal propagation prediction. Numerous models are known for terrestrial systems. They are often complex and too time consuming to achieve a desired degree of accuracy. In terrestrial systems the predicted signal level is nearly constant at a certain location since the base stations are fixed. Due to the dynamics in satellite systems using non-geostationary satellites, the application of such methods is much more time consuming. Efficient methods with sufficient accuracy are needed to predict the signal level for certain locations in a region. In this paper we present methods for generating models of mountainous regions that can be used to estimate the service coverage in modeled region.

II. MODELING OF MOUNTAINOUS REGIONS

Mountains may be modeled by height fields. Height fields are equidistant unit grids in the xy-plane. The node values contain the height values in the z-direction. Planes defined by four neighboring points are called cells. Since the quantity of available data for an investigated region differs, several generation methods are needed. These are,

1. parametric automatic generation,
2. semi-automatic generation based on a few points representing the main geometry, and
3. non-automatic generation using topographical data.

A. Automatic Generation of Terrains

Fractional Brownian surfaces *fBs* are suitable for automatic generation of terrain models. They can be generated by the application of the fractional Brownian motion *fBm* in two dimensions [5]. A *fBm* can be generated by the Gaussian midpoint displacement method [6]. This method is easy to implement and is efficient concerning computation time.

For the Gaussian midpoint displacement method the process $X(t)$ is calculated by halving the time distance between two points successively. A scaled random value is added to the generated half-way-points, Fig. 1. Halving is called k-th refinement. During the k-th refinements 2^{k-1} new points are generated. The k-th refinement is determined from the values of the $(k-1)$-th refinement by

$$X\left(\frac{i}{2^k}\right) = \frac{X\left(\frac{i+1}{2^k}\right) + X\left(\frac{i-1}{2^k}\right)}{2} + D_{ki} S_k \qquad (1)$$

with $i=1,3,5,\ldots,2^k-1$ and $k>0$. D_{ki} are independent Gaussian variables. The scaling factor S_k decreases the magnitude of displacements with increasing k. S_k is determined by

$$S_k = \sqrt{1-2^{2H-2}}\left(\frac{1}{2^{\mathrm{H}}}\right)^{\mathrm{k}\text{-}1} \quad \text{with} \quad 0 < H < 1 \quad \text{and} \quad k > 0. \quad (2)$$

The Hurst exponent H determines the relation between two successive increases and thus the roughness of the *fBm*.

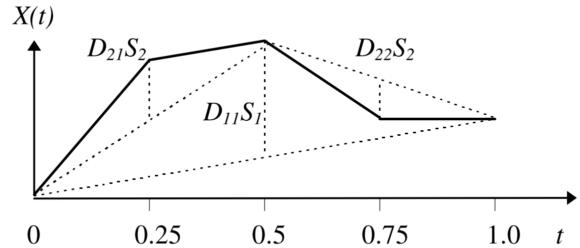

Fig. 1: Gaussian midpoint displacement

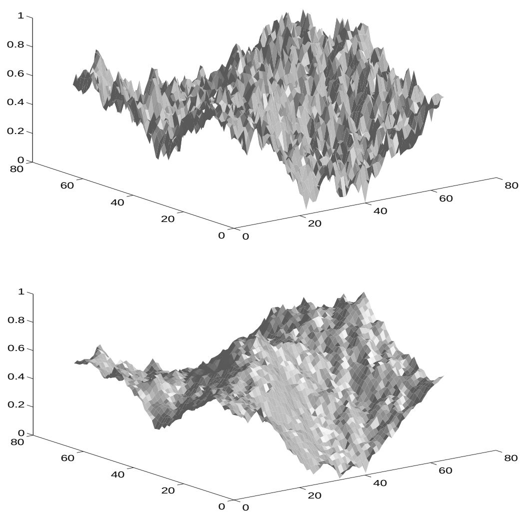

Fig. 2: *fBs* (a) H=0.5, (b) H=0.999

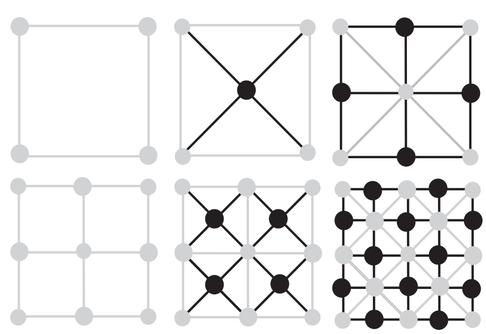

Fig. 3: Midpoint displacement scheme on a square

A fractional Brownian surface *fBs* can be obtained by the application of the *fBm* over a plane. The relations between successive increases of *fBm* are also valid for *fBs* as depicted in Fig. 2. The method for generation of *fBs* is also based on the Gaussian midpoint displacement method. However, now the Gaussian midpoint displacement method is applied to an initial square in two steps, Fig. 3. By arranging a set of initial squares, a terrain model with different ground structures can be generated. While the *fBs* in Fig. 2 are generated from one initial square, the *fBs* in Fig. 4 is generated from 6x4 initial squares.

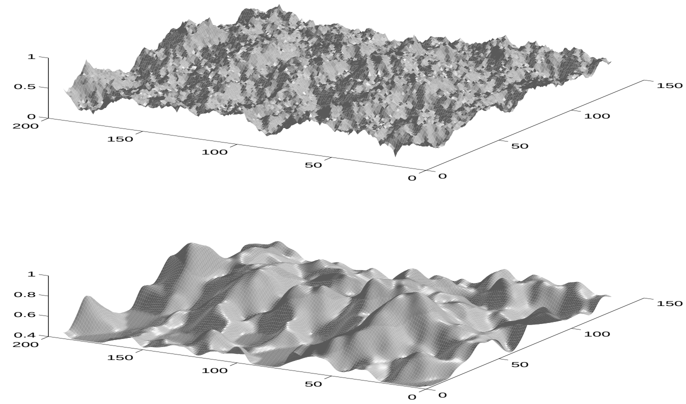

Fig. 4: *fBs* from 6x4 squares with H=0.98
(a) without modifications,
(b) filtered with n=2 and normalized

Fig. 4-a shows that a *fBs* is too irregular for representing mountainous regions without further processing. The surface has to be smoothed and the statistical identity of mountains and valleys has to be removed.

The surface can be smoothed by two-dimensional convolution using the convolution kernel method [7]. The two-dimensional convolution is a two-dimensional digital non-recursive low-pass filter. The outputs of this filter are,

$$\tilde{z}(k,l) = \sum_{i=-n}^{+n} \sum_{j=-n}^{+n} \mathrm{b}_{\mathrm{ij}} z(k-i, l-j) \cdot \quad (3)$$

with

$$b_{ij} \geq 0 \text{ and } \sum_{i=-n}^{+n} \sum_{j=-n}^{+n} b_{ij} = 1$$

$$b_{ij} = \frac{1}{(2n+1)^2} \quad (4)$$

where n is the order of the filter and b_{ij} are the convolution coefficients. For smoothing a *fBs* it is sufficient when all coefficients have the same value (4), see Fig. 4. Filtering is then a moving averaging process. The statistical identity of valleys and mountain peaks can be removed by scaling using non-linear scaling functions, e.g.

$$\tilde{z}_{kl} = f_S(z_{kl}) z_{kl} + f_O(z_{kl}), \quad f_S(z_{kl}) = \begin{cases} 0 & \text{for } z_{kl} < 0.4 \\ 1 & \text{otherwise} \end{cases} \quad (5)$$

$$f_O(z_{kl}) = \begin{cases} 0.4 & \text{for } z_{kl} < 0.4 \\ 0 & \text{otherwise} \end{cases}$$

B. Semi-automatic generation of terrains

If a few points of a region are known, semi-automatic generation may be used. This generation method is a combination of interpolation and *fBs* generation. Given points that characterize the geometry of a region are used for interpolating not specified points in the model. After this interpolation, the model can be refined with small irregularities by using the

Gaussian midpoint displacement method, described above.

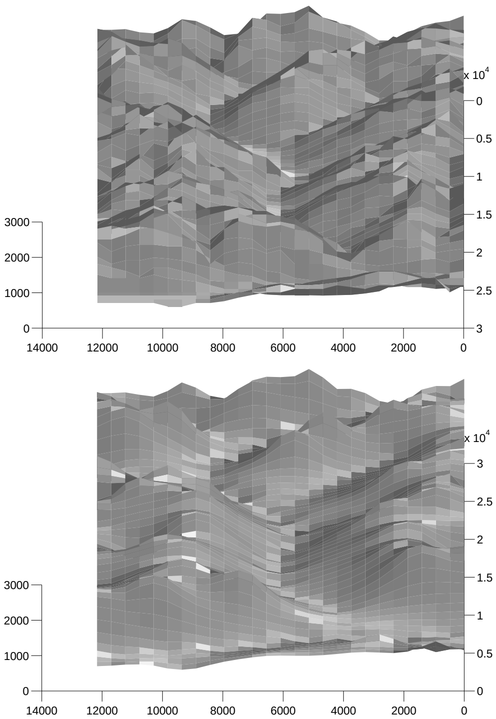

Fig. 5: Models of the Gasteiner Valley
(a) original with 1755 given values
(b) interpolated with 130 values

For interpolation we use the inverse distance weighted interpolation. Although, this method is intuitive and easy to implement, it delivers often satisfying results. An interpolated value $z=f(\boldsymbol{p})$ is determined on a set of given points $(\boldsymbol{p}_i, z_i)$ with $z_i=f(\boldsymbol{p}_i)$ by

$$f(\boldsymbol{p}) = \sum_i w_i(\boldsymbol{p}) f(\boldsymbol{p}_i) \tag{6}$$

$$w_i(\boldsymbol{p}) = \frac{\sigma_i(\boldsymbol{p})}{\sum_j \sigma_j(\boldsymbol{p})} \tag{7}$$

$$\sigma_i(\boldsymbol{p}) = \frac{1}{\left\| \boldsymbol{p} - \boldsymbol{p}_i \right\|_2^{\mu}} \tag{8}$$

with

$$\sum_i w_i(\boldsymbol{p}) = 1 \quad \text{and} \quad w_i(\boldsymbol{p}) \geq 0 \cdot \tag{9}$$

The value of μ specifies the influence of given points dependent on their distance from the interpolated point. Fig. 5 shows the result of an interpolated model of the Gasteiner valley, Alps, in comparison with the original model with equal resolution.

C. Using Topographical Data

In case where topographical data base with desired resolution is available, these data can be used for modeling. Topographical data can be extracted from topographical maps or from GIS (Geographic Information Systems) data bases.

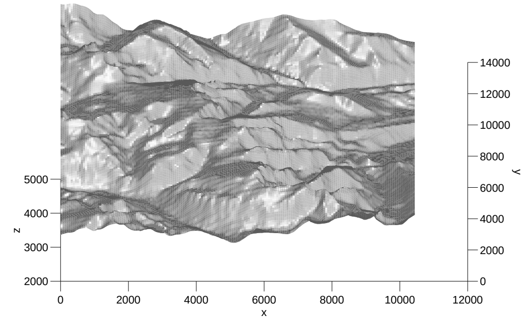

Fig. 6: Mc Henrys Peak, Rocky Mountains

Fig. 6 shows a model of a part of Rocky Mountains. The data base, a so called DEM (Digital Elevation Model) was taken from the US Geographic Survey in public domain. However, at this moment such data bases are not available for the whole world. Existing data bases missing sufficient resolution. Furthermore they are often given in a non-uniform grid, e.g., in a grid of geographical coordinates. Therefore the extraction of region characterizing points from topographical map with subsequent interpolation is often a good way to model a mountainous region with sufficient accuracy.

III. VISIBILITY ANALYSIS IN SATELLITE SYSTEMS WITH MODELED TERRAINS

Due to the power requirements for handheld terminals, the service coverage is strongly dependent on the visibility of satellites. A possible application of modeled terrains is the simulative investigation of the visibility for fast moving satellites.

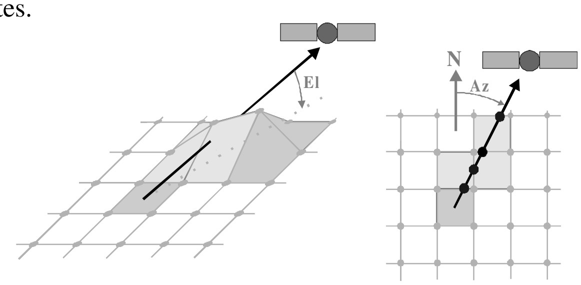

Fig. 7: Schematic representation of grid tracing

A. Visibility Analysis with Grid Tracing

Grid tracing [8], a modified ray tracing algorithm, is a suitable method for visibility analyses. A ray is sent from a given point in terrain in the direction of a given azimuth and elevation. A test for intersection between a cell and the ray is carried out for all cells the ray is traversing, Fig. 7. In case of intersection, the satellite is not visible and the algorithm is terminated. To accelerate this method following condition can be formulated. If

$$\min(z_{R1}, z_{R2}) > \max(z_{i,j}, z_{i,j+1}, z_{i+1,j}, z_{i+1,j+1}), \tag{11}$$

where $z_{i,j}$, $z_{i,j+1}$, $z_{i+1,j}$, $z_{i+1,j+1}$ are the corner points of the cell ij and z_{R1}, z_{R2} are the height of the ray at the cell entry and the cell leaving point, the ray does not intersect the cell. If this condition is not satisfied, the intersection equation between the ray and cell plane has to be solved.

B. Generation of minimum elevation panorama

The described method can also be used to generate an elevation panorama for a certain point in a modeled terrain. For this purpose the grid tracing algorithm was further modified. The ray is sent with elevation of zero degree. If an intersection with a cell occurs, the gradient of the ray is increased so that the height of the ray is equal to the height of the ray in the cell leaving point. The application of this method to all traversed cells results in the minimum elevation angle from a starting point in the given direction.

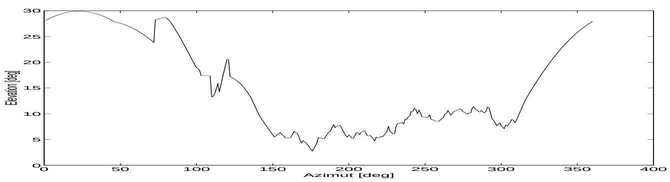

Fig. 8: Elevation panorama in the Gasteiner Valley

C. Visibility simulation results

Described methods were used to analyze the visibility of proposed future satellites systems, Tab. 1 [9, 10, 11, 12, 13], in an example terrain, the Gasteiner valley.

System	Number Satellites	Altitude [km]	Inclination [deg]	Simulation Time[s]
Aries	48	1020	90	13600
Globalstar	48	1406	52	10800
Iridium	66	780	86	10000
Jocus	7	13900	75	86164
LEONET	15	6390	54	4800
MAGSS-14	14	10355	56	82800
Odyssey	12	10354	55	86400
Teledesic	840	700	98.2	2160

Tab. 1: Satellite systems and simulation parameters

For each satellite system the spatial mean and minimum visibilities for at least one, two, three and four satellites were evaluated and are depicted in Fig. 9. Fig. 9-b shows that the minimum visibility for at least one satellite is significantly lower than one for a few systems. In spite of outstanding spatial mean visibility, Fig. 9-a, there are regions in which the visibility for at least one satellite is much lower than the acceptance value of about 95%. The spatial visibility distribution for at least one satellite over the investigated terrain for the Iridium system is depicted in Fig. 11-a.

Further important information, which can be obtained from the simulative investigations with a terrain model, is the distribution of occurrences of temporal gaps in the visibility. For the Iridium system, Fig. 10 shows such a distribution of temporal visibility gaps for a critical location in the example terrain Gasteiner Valley.

For the assumption, that a connection can be maintained over 10 seconds without line of sight to satellite, we can conclude from Fig. 10 that a call of mobile stations is terminated in the investigated location with a probability of about 0.88.

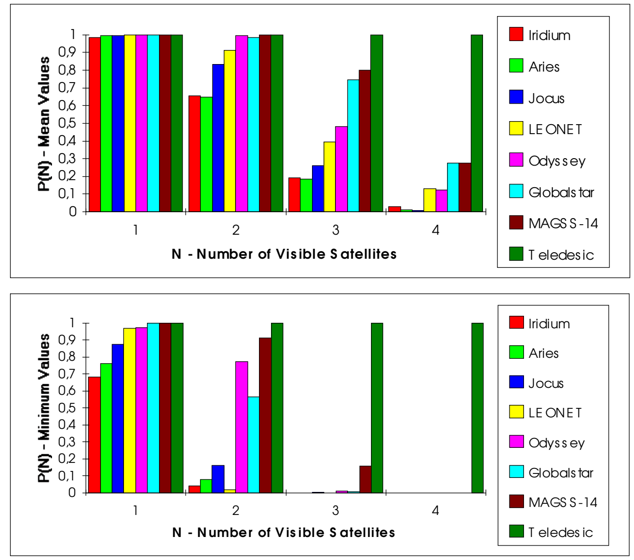

Fig. 9: Mean and minimum visibility for at least one satellite P(N=1)

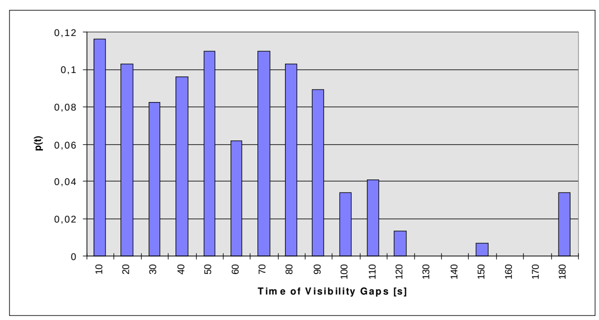

Fig. 10: Empirical distribution of visibility gaps duration

Since satellites in non-geostationary orbits are moving relative to the earth, handover mechanisms are needed. For handovers between satellites, the visibility of at least two satellites is required. For our terrain the analyses of spatial mean visibility for at least two satellites show that only a few of the satellite systems have a sufficient value for the visibility. For systems like the Iridium system, the visibility for at least two satellites is insufficient. From this one can conclude that the Iridium system is not appropriate serving mountainous regions like the example terrain. Fig. 9 shows, the more appropriate systems for the realization of inter-satellite handovers are systems like MAGSS-14 or Teledesic. The realization of full service coverage for mountainous regions with systems like Iridium can only be reached through a careful integration with terrestrial components.

Fig. 11-b shows the results of visibility analysis for the interpolated example terrain. The error in visibilities between simulations based on topographical and interpolated terrain model is depicted in Fig. 11-c. From this we can see that the

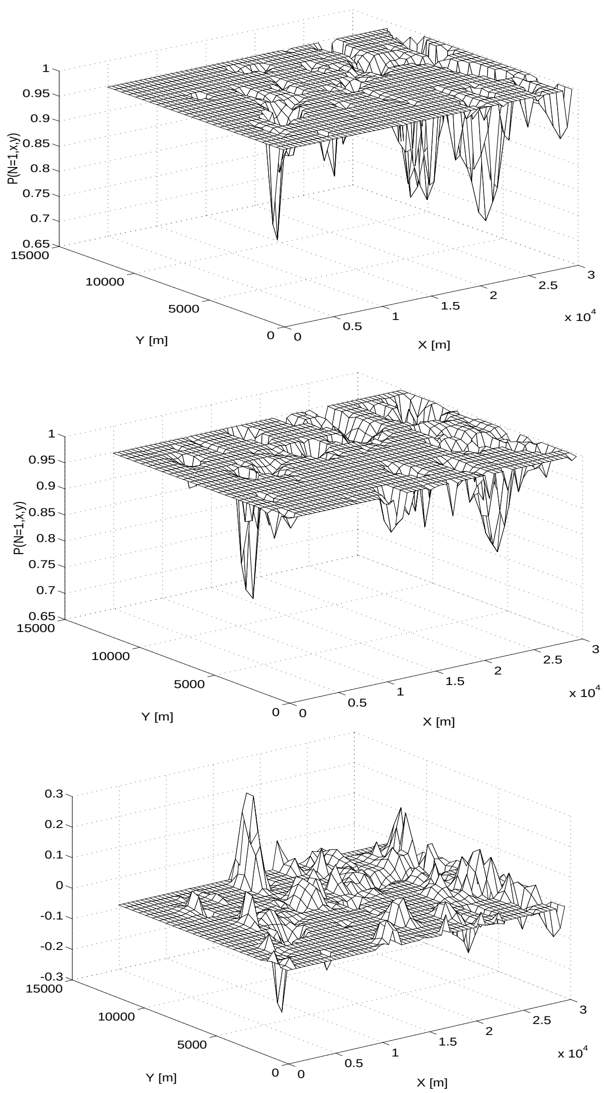

Fig. 11: Visibility P(N=1) for Iridium in the Gasteiner Valley
(a) based on model using topographical data
(b) based on model using interpolation
(c) error between visibilities

IV. CONCLUSIONS

In this paper we presented methods for the generation of terrain models and methods for visibility analysis. Visibility analysis methods based on terrain models can be used to investigate the service coverage in satellite integrated mobile communications systems. Terrain models can also be used for signal level characterization based on two-state channel models as proposed in [2]. Whereas these models use statistics to switch between signal level distribution states dependent on a few classes of terrain, modeled terrains can be used to switch between them more realisticly. Furthermore, simulations with modeled terrains can be used to investigate handover probabilities between satellites and terrestrial components. The results of such investigations are useful during the design phase of an integrated terrestrial and satellite communications system. They permit to develop systems with optimal service coverage also for mountainous regions.

REFERENCES

[1] G. E. Corazza and F. Vatalaro, „*A Statistical Model for Land Mobile Satellite Channels and Its Application to Non-geostationary Orbit Systems,*“ IEEE Trans. Vehic. Technol., vol. VT-43, pp. 738-741, Aug. 1994

[2] E. Lutz, D. Cygan, M. Diepold, F. Dolainsky, and W. Papke, „*The land mobile satellite communication channel,*“ IEEE Trans. Vehic. Technol., vol. VT-40, pp. 375-386, May 1991

[3] A. Jahn, S. Buonomo, M. Sforza, and E. Lutz, „*A Wideband Channel Model for Land Mobile Satellite Systems,*“ Proc. Int. Mobile Satellite Conference IMSC’95, pp. 122-127, Ottawa, June 1995

[4] B. Vucetic and Jun Du, „*Channel Modeling and Simulation in Satellite Mobile Communication Systems,*“ IEEE J. Select. Areas Commun., vol. JSAC-10, pp. 1209-1218, Oct. 1992

[5] B. B. Mandelbrot, „*The Fractal Geometry of Nature,*“ W. H. Freeman, New York 1983

[6] H.-O. Peitgen, H. Jürgens, and D. Saupe, „*Chaos and Fractals: New Frontiers of Science,*“ Springer, New York 1992

[7] C. Watkins, A. Sadun, and S. Marenka, „*Modern Image Processing: Warping, Morphing, and Classical Techniques,*“ Academic Press Professional, Cambridge MA 1993

[8] F. K. Musgrave, „*Grid Tracing: Fast Ray Tracing for Height Fields,*“ Yale Dept. of Computer Science, Research Report RR-639, July 1988

[9] G: Pennoni, „*JOCOS: 6+1 Satellites for Global Mobile Communications,*“ Proc. GLOBCOMM, San Francisco CA 1994

[10] R. J. Rusch, „*Odyssey, an optimized personal communications satellite system,*“ IOS Press space communications, vol. 11(1993), pp. 275-286

[11] E. F. Tuck; et al, „*The Calling Network: a global telephone network,*“ IOS Press space communications, vol. 11(1993), pp. 141-161

[12] ETSI Technical Report, „*Possible European Standardization of Certain Aspects of Satellite Personal Communications Networks (S-PCN),*“ ETSI PT 37V, Apr. 1993

[13] J. Benedicto, J. Fortuny, P. Rastrilla, „*MAGSS-14: A Medium-Altitude Global Mobile Satellite System for Personal Communications at L-Band,*“ ESA Journal, vol. 16, Feb. 1992